Microchimica Acta (2018) 185: 351
https://doi.org/10.1007/s00604-018-2900-9

ORIGINAL PAPER

Colorimetric determination of Hg(II) via the gold amalgam induced deaggregation of gold nanoparticles

Yonghong Xie[1]

Received: 5 May 2018 / Accepted: 28 June 2018 / Published online: 2 July 2018

Abstract

A method is described for the colorimetric determination of mercury(II). In the absence of Hg(II), aminopropyltriethoxysilane (APTES) which is positively charged at pH 7 is electrostatically absorbed on the surface of gold nanoparticles (AuNPs). This neutralizes the negative charges of the AuNPs and leads to NP aggregation and a color change from red to blue-purple. However, in the presence of Hg(II), reduced Hg (formed through the reaction between Hg(II) and citrate on the AuNP surface) will replace the APTES on the AuNPs. Hence, the formation of aggregates is suppressed and the color of the solution does not change. The assay is performed by measuring the ratio of absorbances at 650 and 520 nm and can detect Hg(II) at nanomolar levels with a 10 nM limit of detection. The specific affinity between mercury and gold warrants the excellent selectivity for Hg(II) over other environmentally relevant metal ions.

Keywords Mercury ions · Colorimetric probe · Gold amalgam · Aminopropyltriethoxysilane · Deaggregation · Ratiometric method · Limit of detection · Nanomolar level · Excellent selectivity · Specific affinity

Introduction

Mercury ions (Hg^{2+}) are one of the most toxic heavy metal ions [1, 2]. They can cause serious injury to brain, lungs, kidney, nervous system, immune system, etc [3–6]. In order to protect human beings from the toxic effects of long-term exposure to Hg^{2+}, The World Health Organization (WHO) has defined the maximum level of inorganic mercury in drinking water as 30 nM [7]. Therefore, sensitive and selective detection of Hg^{2+} is very important in monitoring of aqueous environment.

Many methods have been utilized to detect Hg^{2+}, including atomic emission spectroscopy (AES) [8], atomic absorption spectroscopy (AAS) [9, 10], fluorescence [11], inductively coupled plasma mass spectrometry (ICP-MS) [12, 13], and electrochemical method [14, 15]. However, these methods require time-consuming and tedious sample preparation and treatment, and expensive instrumentation, which seriously limit their applications in on-site detection of Hg^{2+}.

Colorimetry is simple and inexpensive, and color changes can be detected visually [16–19]. Nobel metals, especially gold nanoparticles (AuNPs) have used as colorimetric probes for Hg^{2+} detection [20–24] due to unique optical properties known as stronger localizedsurface plasmon resonance (LSPR) and readout distinguishable to the bare eye [25–27]. However, most of AuNP surface needs to be modified with specific surface functionalized molecules for selective interaction with Hg^{2+}. In addtion to strong interaction with Hg^{2+}, these AuNP surface functionalized molecules also interact with other transition metal ions, affecting the selectivity.

To solve the above issue, herein, we present a highly selective colorimetric method for Hg^{2+} detection based on gold amalgam-induced deaggregation of AuNPs in the presence of aminopropyltriethoxysilane (APTES). The APTES molecules absorbed on the surface of AuNPs destabilize the dispersion state of AuNPs,

Electronic supplementary material The online version of this article (https://doi.org/10.1007/s00604-018-2900-9) contains supplementary material, which is available to authorized users.

✉ Yonghong Xie
xieyonghongnjnu@sina.com

[1] College of Chemistry and Chemical Engineering, Neijiang Normal University, Neijiang 641100, Sichuan, China

leading to a distinct color change from red to blue-purple. Interestingly, in the presence of different concentrations of Hg^{2+}, the formation of gold amalgam makes that reduced Hg occupy the former location of APTES, and prevents AuNPs from aggregation, resulting in a blue-purple-to-red color change. The concentration dependent color and absorbance changes suggest that the assay can detect Hg^{2+} up to nanomolar level.

Experimental section

Materials

Hydrogen tetrachloroaurate trihydrate ($HAuCl_4 \cdot 3H_2O$, 99.9%), trisodium citrate, APTES, and Tris-base were purchased from Sigma-Aldrich. All other chemicals are of analytical reagent grade. Ultrapure water obtained from a Millipore water purification system (>18.2 MΩ cm, Milli-Q, Millipore) was used in all assays and solutions. All glasswares were cleaned with freshly prepared aqua regia and rinsed thoroughly with DI water prior to use.

Apparatus

UV-vis spectra were recorded using a U-3900 UV-vis spectrophotometer and processed using OriginLab software (Hitachi, Japan). The size and morphology of AuNPs were observed with a Hitachi H-7500 transmission electron microscope (TEM, Tokyo, Japan).

Synthesis of AuNPs [28]

AuNPs with an average diameter of 13 nm were prepared through the previous reported method (Supporting Information).

Detection of Hg^{2+}

10 μL of various concentrations of Hg^{2+} solutions (final concentration: 15.4, 46.2, 61.5, 76.9, and 92.3 nM) was added into 540 μL AuNP solution (2.5 nM), respectively. After reaction for 1.5 h, 70 μL of 20 mM Tris-HCl buffer (pH 7.2) was separately added into the mixtures. Then, 30 μL 4.2 mM APTES was injected into the above solutions for 20 min of incubation at room temperature. Finally, the solutions were used for absorbance measurement at a wavelength of 520 and 620 nm.

Results and discussion

Detection principle

Scheme 1 shows the schematic illustration of the Hg^{2+} assay. In the absence of target Hg^{2+}, APTES molecules were absorbed onto the surfaces of AuNPs via Au-NH_2 bonds. The positive charges of APTES weakened the negative charges of AuNPs, leading to the AuNP aggregation. The solution color quickly changed from red to blue-purple. While in the presence of target Hg^{2+}, citrate ions attached to the AuNP surfaces reduced Hg^{2+} to Hg, and then formed the gold amalgam deposited onto the surfaces of AuNPs. The formation of the gold amalgam may effectively inhibit the accessibility of APTES molecules to the surfaces of AuNPs, and prevented the aggregation of AuNPs. The solution underwent the color change from blue-purple-to-red, thus deaggregation of AuNPs resulted in a bare eye-based assay for Hg^{2+}.

Optimization of detection conditions

To achieve an optimal sensing performance, the experimental conditions including APTES concentration, solution pH, and reaction time between Hg^{2+} and AuNPs were examined. Fig. S1A shows the absorbance change (K_0/K) of the solution toward APTES with varying concentrations in the presence of 1 μM Hg^{2+}, where K_0 and K were the absorbance ($K = A_{620\ nm}/A_{520\ nm}$) of the AuNP solution in the absence and presence of the target Hg^{2+}, respectively. As seen from Fig. S1A, K_0/K increased with the increasing Hg^{2+} concentration (66.7-193.8 μM) and then decreased after 193.8 μM. Therefore, a Hg^{2+} concentration of 193.8μM was used for the following experiment. Next, we investigated the optimum reaction between Hg^{2+} and AuNPs in the assay. Fig. S1B shows that the leaping range in K_0/K occurred in 1.5 h, it was all downhill after 1.5 h. Thus, the optimal reaction time was 1.5 h. The pH value of the solution was also a key factor that affected the sensitivity of the assay. In this case, solutions with various pH values (4-8) were used to investigate the performance of the assay. As shown in Fig. S1C, the maximum K_0/K was obtained when pH was 7.2. However, higher pH caused the decrease of K_0/K. Thus, all subsequent experiments were conducted at pH 7.2.

Colorimetric detection of Hg^{2+}

Pursuant to characterizing the sensitivity and the limit of detection (LOD) of the assay for Hg^{2+}. The UV-vis

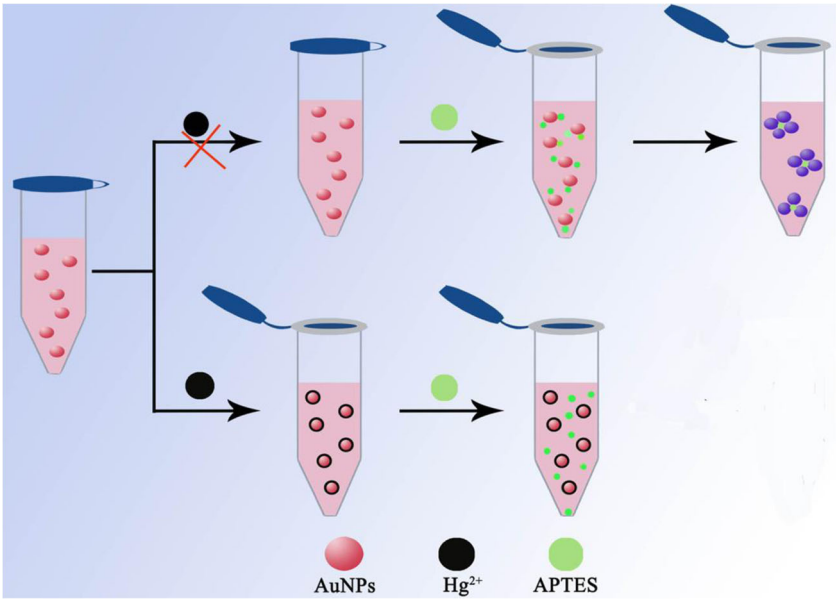

Scheme 1 Schematic illustration of colorimetric detection of Hg^{2+} based on gold amalgam-induced deaggregation of AuNPs

absorption spectra of AuNP solutions were recorded after adding various concentrations of Hg^{2+} under the optimized conditions. As shown in Fig. 1a, the absorbance decreased with the increment of Hg^{2+} (0-92.3 nM). An obvious color change from blue-purple to red was observed with the increase of target Hg^{2+} concentration in the solution (inset of Fig. 1b). Also, a linear relationship between the absorption ratio ($A_{620\ nm}/A_{520\ nm}$) and the Hg^{2+} level (0-92.3 nM) was obtained (Fig. 1b). The LOD was 10 nM estimated by the 3σ rule, which was lower than the guideline Hg^{2+} concentration of (30 nM) in drinking water set by the WHO. Compared with other methods for Hg(II) detection, as shown in Table 1, the sensitivity of our method was comparable or more sensitive. Furthermore, the other direct evidence for the deaggregation of AuNPs induced by the addition of Hg^{2+} was confirmed by the TEM measurement. As shown in Fig. 2, the AuNPs underwent an aggregation-dispersion process in the presence of target Hg^{2+}.

Selectivity of the assay

An essential feature of a metal ion assay is its selectivity not only to isolated metal ions but also to mixtures that are environmentally relevant. We tested 8 individual metal ions including Sn^{2+}, Mn^{2+}, Na^{+}, Cd^{2+}, Co^{2+}, Zn^{2+}, Pb^{2+}, and Fe^{2+} at a concentration of 1 μM, and the mixture of the 8 metal ions. As shonwn in Fig. 3, the interference from the 8 metal ions and the mixture only caused a slight decrease in the absorbance, whereas 0.1μM Hg^{2+} gave rise to a tremendous decrease, compared with that of the background. Furthermore, the corresponding color photographs also show that only Hg^{2+} caused a blue-purple-to-red color change while

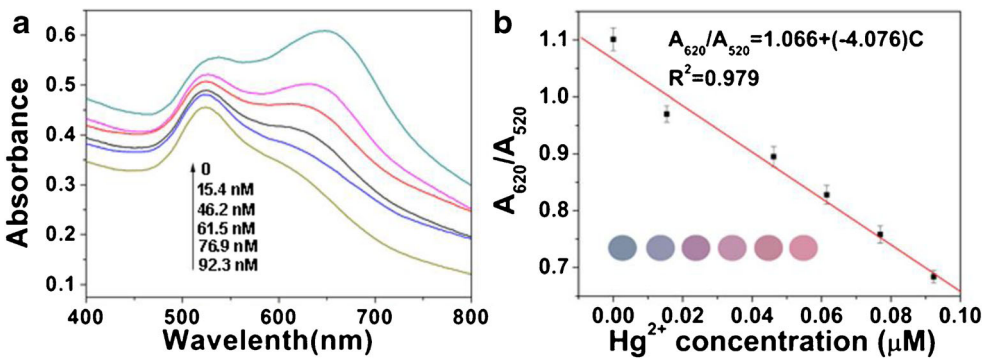

Fig. 1 **a** UV-vis spectra of the solutions response for the Hg^{2+} concentration (0-92.3 nM). **b** Plot of $A_{620\ nm}/A_{520\ nm}$ *vs* Hg^{2+} concentration (0-92.3 nM). Error bars indicate standard deviation of the mean of three experiments

Table 1 Comparison of our approach with other reported methods for Hg(II) detection

Material	Method	Detection limit	Linear range	Ref.
AuNPs, APTES	colorimetric	10 nM	0-92.3 nM	this work
Fe_3O_4@SiO_2@graphene quantum dot	fluorescent	30 nM	0.1-70 μM	[29]
Silver-doped CdS quantum dots	colorimetric	124 μM	0.1-1.2 mM	[30]
DNA, AuNPs	colorimetric	3.4 nM	5 nM-10 μM	[23]
carbon dots and CdTe quantum dots	fluorescent	0.47 nM	0.47-50 nM	[31]
silver nanoparticles	colorimetric	125 nM	0.625- 5 μM	[32]
gold nanorods	colorimetric	0.48 nM	1-100 nM	[33]

other environmentally relevant metal ions remained blue-purple. Obviously, the interference of these metal ions to the assay was negligible. The excellent selectivity can be attributed to the specific interaction of gold with Hg^{2+}.

The practicality of this assay

To explore whether the method was feasible to real samples, the practicality of Hg^{2+} detection in river water samples using the method was tested. The river water was collected from city moat (Beijing, China) and filtered through 0.22 μM nitrocellulose membranes to remove physical impurities. There was no detectable Hg^{2+} existing in the river water samples analyzed by ICP-MS. Therefore, employing the standard addition method, Hg^{2+} was respectively spiked into river water samples at different concentrations (15.4, 30.8, 46.2, 61.5, and 76.9 nM) and then measured with our method. As shown in Fig. 4a, it is seen that the absorbance decreased with the Hg^{2+} concentration increasing from 0 to 92.3 nM. The calibration curve for detecting Hg^{2+} in river water samples was obtained by plotting the values of ($A_{620\ nm}/A_{520\ nm}$) versus Hg^{2+} concentrations (0-92.3 nM) (Fig. 4b). In spite of the interference from organics and many minerals existing in river water, the results from the river samples were in good agreement with those from Tris-HCl buffer, indicating that the assay can satisfy the practical determination of Hg^{2+} in real samples.

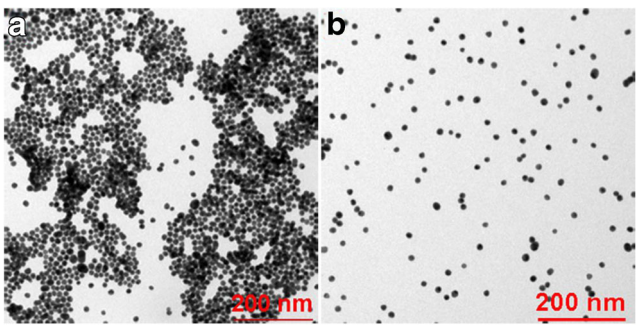

Fig. 2 TEM images of AuNPs in the (**a**) absence and (**b**) presence of 92.3 nM Hg^{2+} in the presence of 0.2 mM APTES

Conclusion

In summary, we have demonstrated a sensing strategy to be utilized for the determination of Hg^{2+} in aqueous solution. In the sensing system, target Hg^{2+} absorbed on the surfaces of citrate-capped AuNPs was reduced to Hg, the specific interaction between Au and Hg to form gold amalgam was employed to prevent the AuNP aggregation in the presence of APTES. The aggregation-to-deaggregation change can be easily accomplished by the bare eyes or UV-vis spectrometer. The method can provide a LOD of 10 nM with outstanding selectivity in mixed solutions containing eight other metal ions. Moreover, the experiments for detection of Hg^{2+} in river water had been demonstrated with satisfactory results. The limitation of the study is that the sensitivity needs to be further improved.

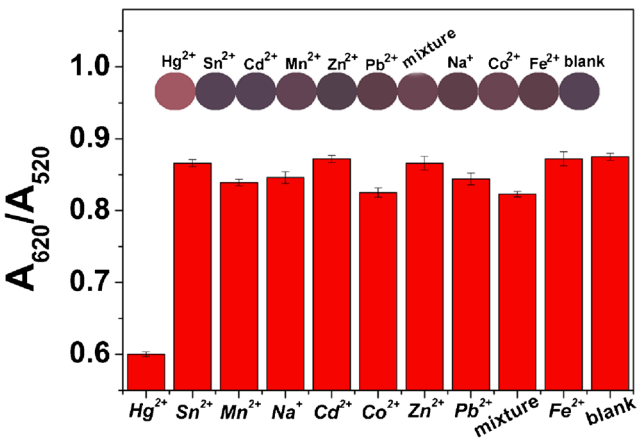

Fig. 3 The absorption ratio ($A_{620\ nm}/A_{520\ nm}$) change for Hg^{2+} and other environmentally relevant metal ions. Inset: color changes of the solution in the presence of 0.1μM Hg^{2+} and 8 individual metal ions and the mixture of the 8 metal ions, each at 1 μM. Error bars indicate standard deviation of the mean of three experiments

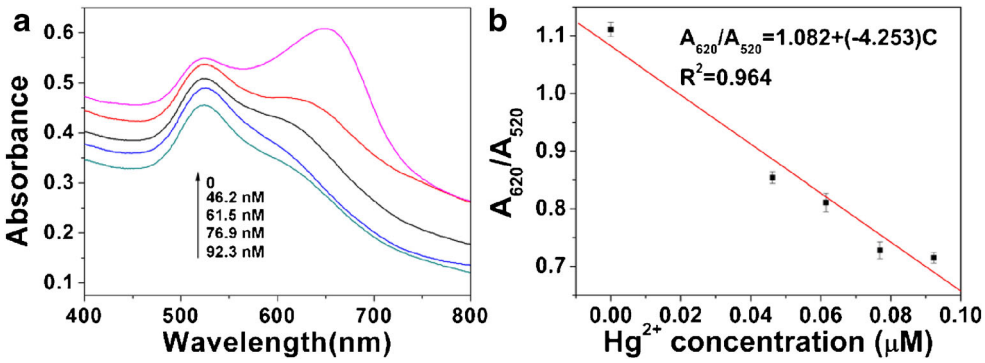

Fig. 4 **a** UV-visible spectra of AuNP solution in the presence of various Hg^{2+} concentrations (from top to bottom: 0, 46.2, 61.5, 76.9, and 92.3 nM) in river water. **b** The dependence of $A_{620\ nm}/A_{520\ nm}$ on the Hg^{2+} concentrations in the range of 0-92.3 nM. Error bars indicate standard deviation of the mean of three experiments

Compliance with ethical standards The author(s) declare that they have no competing interests.

References

1. Bings NH, Bogaerts A, Broekaert JAC (2006) Atomic spectroscopy. Anal. Chem. 78:3917–3945
2. Nolan EM, Lippard SJ (2008) Tools and tactics for the optical detection of mercuric ion. Chem. Rev. 108:3443–3480
3. Fan Y, Long YF, Li YF (2009) A sensitive resonance light scattering spectrometry of trace Hg^{2+} with sulfur ion modified gold nanoparticle. Anal. Chim. Acta 653:207–211
4. Wang Y, Yang F, Yang XR (2010) Colorimetric biosensing of mercury(II) ion using unmodified gold nanoparticle probes and thrombin-binding aptamer. Biosens. Bioelectron. 25:1994–1998
5. Onyido I, Norris AR, Buncel E (2004) Biomolecule-mercuryinteractions: modalities of DNA base-mercury binding mechanisms. Remediation strategies. Chem. Rev. 104:5911–5929
6. Kim HN, Ren WX, Kim JS, Yoon J (2012) Fluorescent and colorimetric sensors for detection of lead, cadmium, and mercury ions. Chem. Soc. Rev. 41:3210–3244
7. Burin GJ, Becking GC (1991) The World-Health-Organization (WHO) guidelines for drinking-water quality: a global perspective on trace contaminants of dinking-water. Trace Substances in Environmental Health-*XXIV* 207-219.
8. Han FX, Dean Patterson W, Xia YJ, Maruthi Sridhar BB, Su YJ (2006) Rapid determination of mercury in plant and soil samples using inductively coupled plasma atomic emission spectroscopy, a comparative study. Water Air SoilPollut. 170:161–171
9. Leermakers M, Baeyens W, Quevauviller P, Horvat M (2005) Mercury inenvironmental samples: speciation, artifacts and validation, Trends Anal. Chem. 24:383–393
10. Kopysc E, Pyrzynska K, Garbos S, Bulska E (2000) Determination of mercury by cold-vapor atomic absorption spectrometry with preconcentration on a gold-trap. Anal. Sci. 16:1309–1312
11. Tianyu H, Xu Y, Weidan N, Xingguang S (2016) Aptamer-based aggregation assay for mercury(II) using gold nanoparticles and fluorescent CdTe quantum dots. Microchimica Acta 183:2131–2137
12. Fong B, Mei W, Siu TS, Lee J, Sai K, Tam S (2007) Determination of mercury inwhole blood and urine by inductively coupled plasma mass spectrometry. J. Anal. Toxicol. 31:281–287
13. Li Y, Chen C, Li B, Sun J, Wang JX, Gao YX, Zhao YL, Chai ZF (2006) Elimination efficiency of different reagents for the memory effect of mercury using ICP-MS. J. Anal. At. Spectrom. 21:94–96
14. Zhu H, Zhang S, Li M, Shao Y, Zhu Z (2010) Electrochemical sensor for melamine based on its copper complex. Chem. Commun. 46:2259–2261
15. Zhang ZP, Tang AA, Liao SZ, Chen PF, Wu ZY, Shen GL, Yu RQ (2011) Oligonucleotide probes applied for sensitive enzyme-amplified electrochemical assay of mercury(II) ions. Biosens. Bioelectron. 26:3320–3324
16. Ding YN, Yang BC, Liu H, Liu ZX, Zhang X, Zheng XW, Liu QY (2018) FePt-Au ternary metallic nanoparticles with the enhanced peroxidase-like activity for ultrafast colorimetric detection of H_2O_2. Sens. Actuators, B 2018(259):775–783
17. Liu QY, Yang YT, Li H, Zhu RR, Shao Q, Yang SG, Xu JJ (2015) NiO nanoparticles modified with 5,10,15,20-tetrakis(4-carboxyl pheyl)-porphyrin: Promising peroxidase mimetics for H_2O_2 and glucose detection. Biosens. Bioelectron. 64:147–153
18. Zhang LY, Chen MX, Jiang YL, Chen MM, Ding YN, Liu QY (2017) A facile preparation of montmorillonite-supported copper sulfide nanocomposites and their application in the detection of H_2O_2. Sens. Actuators, B 239:28–35
19. Sun LF, Ding YY, Jiang YL, Liu QY (2017) Montmorillonite-loaded ceria nanocomposites with superior peroxidase-like activity for rapid colorimetric detection of H_2O_2. Sens. Actuators, B 239: 848–856
20. Hong M, Zeng B, Li M, Xu X, Chen G (2018) An ultrasensitive conformation-dependent colorimetric probe for the detection of mercury(II) using exonuclease III-assisted target recycling and gold nanoparticles. Microchimica Acta 185:72
21. Shamsipur M, Safavi A, Mohammadpour Z, Ahmadi R (2016) Highly selective aggregation assay for visual detection of mercury ion based on competitive binding of sulfur-doped carbon nanodots to gold nanoparticles and mercury ions. Microchimica Acta 183: 2327–2335
22. Zarlaida F, Adlim M (2017) Gold and silver nanoparticles and indicator dyes as active agents in colorimetric spot and strip tests for mercury(II) ions: a review. Microchimica Acta 184:45–58
23. Liu S, Leng X, Wang X, Pei Q, Cui X, Wang Y, Huang J (2017) Enzyme-free colorimetric assay for mercury(II) using DNA conjugated to gold nanoparticles and strand displacement amplification. Microchimica Acta 184:1969–1976
24. Chen ZB, Zhang CM, Tan Y, Zhou TH, Ma H, Wan CQ, Lin YQ, Li K (2015) Chitosan-functionalized gold nanoparticles for colorimetric detection of mercury ions based on chelation-induced aggregation. Microchim Acta 182:611–616
25. Du J, Zhu B, Peng X, Chen X (2014) Optical reading of contaminants in aqueous media based on gold nanoparticles. Small 10: 3461–3479
26. Song Y, Wei W, Qu X (2011) Colorimetric biosensing using smart materials. Adv. Mater. 23:4215–4236
27. Saha K, Agasti SS, Kim C, Li X, Rotello VM (2012) Gold nanoparticles in chemical and biological sensing. Chem. Rev. 112:2739–2779
28. Turkevich J, Stevenson PC, Hillier J (1951) A study of the nucleation and growth processes in the synthesis of colloidal gold. Discuss. Faraday Soc. 11:55–75

29. Alvand M, Shemirani F (2017) A Fe_3O_4@SiO_2@graphene quantum dot core-shell structured nanomaterial as a fluorescent probe and for magnetic removal of mercury(II) ion. Microchim Acta 184: 1621–1629
30. Butwong N, Kunthadong P, Soisungnoen P, Chotichayapong C, Srijaranai S, Luong John HT (2018) Silver-doped CdS quantum dots incorporated into chitosan-coated cellulose as a colorimetric paper test stripe for mercury. Microchimica Acta 185:126
31. Xu HY, Zhang KN, Liu QS, Liu Y, Xie MX (2017) Visual and fluorescent detection of mercury ions by using a dually emissive ratiometric nanohybrid containing carbon dots and CdTe quantum dots. Microchim Acta 184:1199–1206
32. Zhan L, Yang T, Zhen SJ, Huang CZ (2017) Cytosine triphosphate-capped silver nanoparticles as a platform for visual and colorimetric determination of mercury(II) and chromium(III). Microchim Acta 184:3171–3178
33. Bi N, Hu MH, Xu J, Jia L (2017) Colorimetric determination ofmercury(II) based on the inhibition of the aggregation of gold nanorods coated with 6-mercaptopurine. Microchim Acta 184: 3961–3967